REGULAR ARTICLE

blood advances

Blockade of CCR1 induces a phenotypic shift in macrophages and triggers a favorable antilymphoma activity

Kang Le,[1,*] Jing Sun,[1,*] Javid Ghaemmaghami,[1] Mitchell R. Smith,[2] W. K. Eddie Ip,[3] Tycel Phillips,[4] and Mamta Gupta[1]

[1]Department of Biochemistry and Molecular Medicine, George Washington University, George Washington University's Cancer Center (GWCC), Washington DC; [2]Department of Medicine, School of Medicine and Health Sciences, George Washington University, GWCC, Washington DC; [3]Department of Immunology, Mayo Clinic, Rochester, MN; and [4]Department of Hematology, University of Michigan, Ann Arbor, MI

Key Points

- CCR1, expressed on macrophages, promotes macrophage migration and M2-polarization via tumor-derived CCL3.
- CCR1 inhibition exerts antilymphoma activity by reprogramming macrophages.

Tumor-associated macrophages (TAMs) within the tumor microenvironment (TME) play an important role in tumor growth and progression. TAMs have been involved in producing immunosuppressive TME via various factors; however, the underlying mechanisms remain unclear in B-cell lymphoma, including mantle cell lymphoma (MCL). We identified that chemokine receptor-1 (CCR1) is highly expressed on monocytes (Mo) and macrophages (MΦ), and CCR1 pharmacological inhibition or CCR1 siRNA abolished lymphoma-mediated Mo/MΦ migration in a chemotaxis assay. The deficiency of host CCR1 (*CCR1 KO*) was associated with decreased infiltration of peritoneal-MΦ compared with WT-CCR1. Functional studies indicated that the genetic depletion of CCR1 or treatment inhibited protumor MΦ (M2-like) phenotype by decreasing CD206 and IL-10 expression. Moreover, CCR1 depletion reprogrammed MΦ toward an $MHCII^+/TNF\alpha^+$ immunogenic phenotype. Mechanistically, protumor MΦ driven–IL-10 provides a positive feedback loop to tumor-CCL3 by regulating the CCL3 promoter via STAT1 signaling. Therapeutic in vivo targeting of CCR1 with CCR1 antagonist BX-471 significantly reduced FC-muMCL1 mouse tumors in the syngeneic MCL model by the depletion of M2-TAMs and increased infiltration of cytotoxic $CD8^+$ T cells. Our study established that CCR1 exerts a pivotal role in macrophage programming, thus shaping protumor TME and lymphoma progression. CCR1 inhibition through CCR1 antagonists may be a promising therapeutic strategy to reprogram macrophages in lymphoma-TME and achieve better clinical outcomes in patients.

Introduction

Mantle cell lymphoma (MCL) is an incurable subtype of non-Hodgkin lymphoma (NHL) with a tendency for early relapse and worse long-term survival compared with other B-cell malignancies, and the clinical behavior of MCL is variable, with cases ranging from not requiring therapy for years to highly aggressive MCL with limited prognosis.[1] MCL comprises ~5% to 10% of all NHL with a median overall survival rate of 4 to 5 years and frequent relapses.[2,3] Initial treatment broadly consists of a combination of chemotherapy and rituximab, including high-dose cytarabine followed by autologous stem cell

Submitted 5 August 2022; accepted 14 December 2022; prepublished online on *Blood Advances* First Edition 11 January 2023. https://doi.org/10.1182/bloodadvances.2022008722.

*K.L., and J.S. are joint first authors.

Sequencing data can be found in supplemental Table 5.

Data are available on request from the corresponding author, Mamta Gupta (magupta@gwu.edu).

The full-text version of this article contains a data supplement.

transplant in patients fit to receive the treatment.[4-6] Targeted therapy with novel agents such as lenalidomide, ibrutinib, and venetoclax has shown some efficacy in the treatment of relapsed and more recently first-line MCL.[7-9] The resistant disease develops, however, with any of these treatments.[10] A better understanding of the molecular pathogenesis of MCL is thus necessary to establish novel therapies for this "hard to treat" lymphoma. Recent advances have highlighted the critical role of the tumor microenvironment (TME) in tumor progression and response to the therapy.[11-14] The TME is composed of tumoral cells, stromal cells, and immune cells (including monocytes/macrophages, and neutrophils).[15] In various malignancies, increased infiltration of TAMs has been associated with worse prognosis.[16] In solid cancers, TAMs are polarized into the M2-phenotype with protumor function. Infiltrating MΦ have been noted in MCL lymph nodes,[17,18] but their characterization and significance has not been well studied. Recently, we confirmed the presence of M2-TAMs in MCL in an in vivo MCL mouse model.[19] However, the molecular drivers/regulators of macrophage infiltration and macrophage programming in the MCL-niche during MCL progression remain uncertain.

Chemokines are one of the key factors that regulate the migration of immune cells via binding to their receptors.[20,21] Chemokines also contribute to the pathogenesis of several diseases,[22,23] in particular, CCL3 (MIP-1-alpha) plays a role in multiple myeloma (MM) by stimulating migration and proliferation of MM cells.[24] High expression of MCP-1 and CCR2 predicts worse outcomes in diffuse large B-cell lymphoma,[25] and CCR1 is a major receptor on osteoclasts and a novel therapeutic target for osteolytic bone disease in MM.[26,27] The potential role of CCL3 or its receptor CCR1 in macrophage programming in lymphoma-TME has not been evaluated yet. In this study, we sought to determine the unique role of CCR1 as a regulator of macrophage programming in the MCL-TME, and then the therapeutic potential of targeting that CCR1-receptor axis in vivo for MCL. Such insights could be critical for designing more effective therapies and improving clinical responses to B-cell lymphoma.

Materials and methods

Primary MCL patient samples and plasma

Patient material (circulating MCL cells and plasma) was obtained from the patients with mantle cell lymphoma after informed consent was obtained according to a protocol approved by review boards and the ethical committee of the University of Michigan Rogel Cancer Center. Peripheral blood (PB) MCL patient mononuclear cells and MCL plasma were collected from untreated patients. PB MCL cells were isolated after using the Ficoll-Hypaque separation method and stored in liquid nitrogen. PB MCL cells were further separated from mononuclear cells using antihuman–CD19-conjugated magnetic beads with purity >90%. Matched plasma was collected via venipuncture in an ethylenediamine tetraacetic acid (EDTA)-containing tube. Normal human plasma was purchased from Innovative Research (Novi, MI).

Human and murine cell lines

Human MCL cell lines, Mino, Granta, and JVM2 were obtained from the American Type Culture Collection (ATCC) (Manassas, VA). Murine MCL cell line FC-muMCL1 was used as described earlier.[28] Monocytic cell lines THP1, U937, and RAW264.7 were obtained from ATCC. All the cell lines used were cultured in RPMI-1640 with 10% fetal bovine serum (FBS), 1 mM L-glutamine, and penicillin/streptomycin. The cell lines were authenticated by STR Profiling performed at ATCC and Genetica (Burlington, NC).

Antibodies and reagents

Antibodies against STAT1, phospho-STAT1, and GAPDH were purchased from Cell Signaling Technology (MA). Neutralizing antibodies to CCL2, CCL3, CCL4, CCL5, and IL-10, were purchased from the R&D system (MN). Recombinant cytokines IL-10 (#200-10), CCL3 (#300-08), human-MCSF (#300-25), and murine-MCSF (315-02) were purchased from PeproTech (NJ). CCR5 antagonist (Maraviroc), CCR4 antagonist (AZD2098), and CCR1 antagonist (BX-471) were purchased from Med ChemExpress (NJ). STAT1 inhibitor fludarabine was purchased from Selleckchem (Houston, TX).

Human and murine macrophage differentiation

The bone marrow (BM) cells were harvested from femurs and tibias of C57/BL6, *CCR1 KO,* or *IL-10 KO* mice to generate BM–derived macrophages (BMDM). Briefly, the bone's inner cavity was rinsed with PBS followed by centrifugation at 400 x g for 10 minutes. The BM cells were resuspended in RPMI 1640 containing 10% FBS and treated with either 25 ng/mL rM-CSF or 30% L929-conditional media (CM) for 7 days, and the medium was changed every 3 days. To trigger in vitro differentiation of human monocytes, $CD14^+$ monocytes (Mo) derived from peripheral blood mononuclear cells (PBMCs) were treated with rM-CSF (50 ng/mL) for 5 to 7 days, and the medium was supplemented every 2 to 3 days.

Chemotaxis assay

A chemotaxis assay was performed as per the previous study.[29] Briefly, MCL-CM or media (serum-free) alone were used to attract Mo by chemotaxis assay. First, $CD14^+$ Mo, U937-Mo, or THP1-Mo was labeled with calcein AM (5 μg/mL; Invitrogen) for 30 minutes at 37°C. Labeled Mo (1.0×10^6 in 100 μL total volume) was then placed in the top chamber of a 5-μm transwell and medium alone or MCL-CM (600 μL) was placed at the bottom of each well and plates were incubated at 37°C. After a 3-hour chemotaxis assay, transwells were removed and migrated cells in the lower chamber were collected, seeded in 96 well plates, and measured using a multiwell fluorescent plate reader (SepctraMax i3x). Relative migration was calculated using the reading from the medium-alone group as the denominator.

Enzyme-linked immunosorbent assays (ELISA)

ELISA was performed using a human interleukin-10 or human MIP-1α ELISA kit (Invitrogen, CA) as per instructions. Absorbance was measured at 450 nm using a spectrophotometer.

Immunofluorescence

Formalin-fixed paraffin-embedded tissue slides from mouse lymphomas were used for immunofluorescence (IF) as described earlier.[19] The antibodies used for immunofluorescence are listed in supplemental Table 1A.

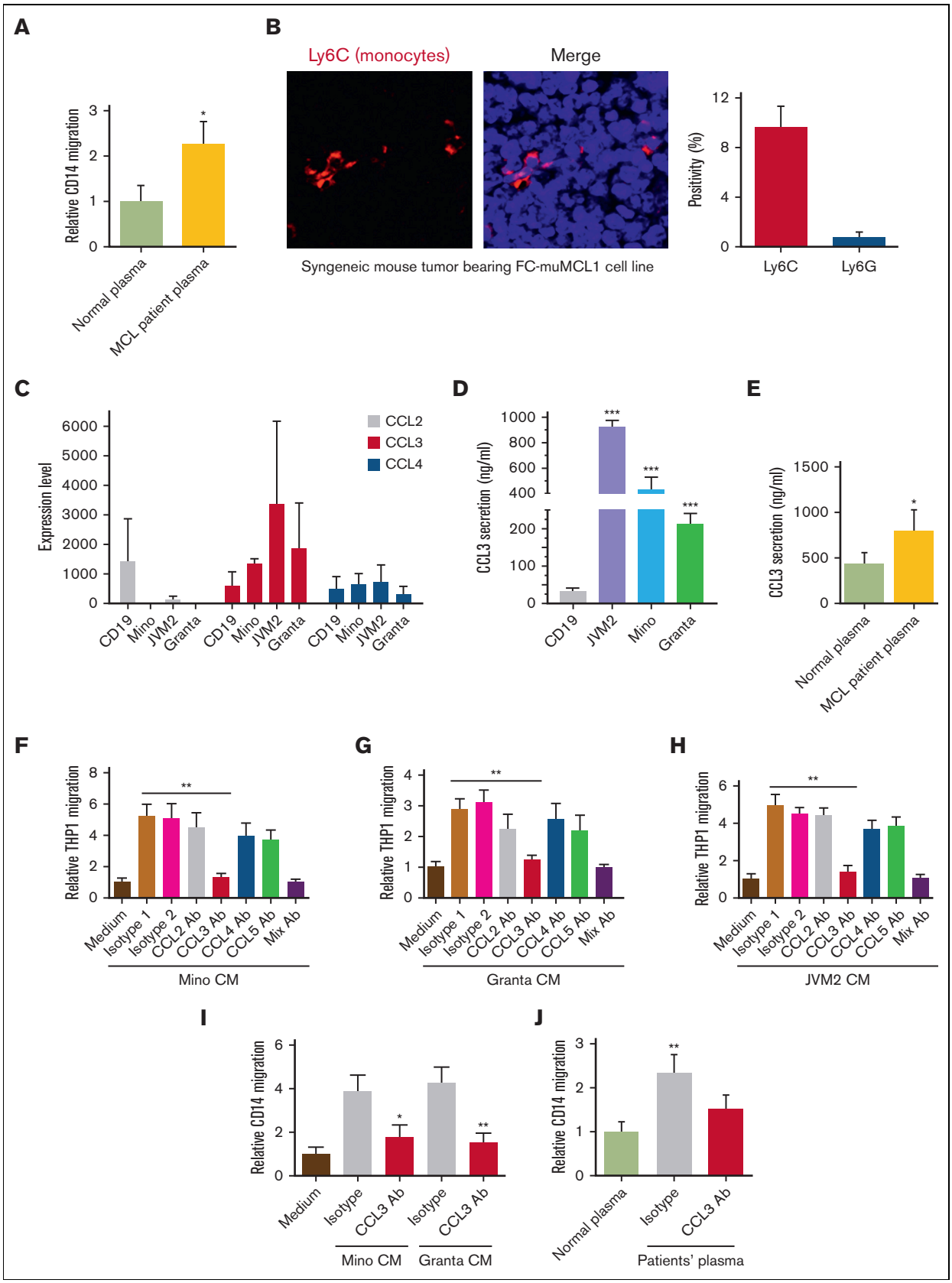
A
Relative CD14 migration
Normal plasma
MCL patient plasma
B
Ly6C (monocytes)
Merge
Syngeneic mouse tumor bearing FC-muMCL1 cell line
Positivity (%)
Ly6C
Ly6G
C
Expression level
CCL2
CCL3
CCL4
CD19
Mino
JVM2
Granta
D
CCL3 secretion (ng/ml)
E
CCL3 secretion (ng/ml)
Normal plasma
MCL patient plasma
F
Relative THP1 migration
Medium
Isotype 1
Isotype 2
CCL2 Ab
CCL3 Ab
CCL4 Ab
CCL5 Ab
Mix Ab
Mino CM
G
Granta CM
H
JVM2 CM
I
Relative CD14 migration
Medium
Isotype
CCL3 Ab
Mino CM
Granta CM
J
Normal plasma
Patients' plasma

Figure 1.

Flow cytometry

All the analyzed flow cytometry sets used LIVE/DEAD Aqua or Sytox Red stain (Thermo Fisher, MA), with matched isotype antibodies as controls. The first set was performed to assess surface markers using antibodies against CCR1 and CCR5. The cells were harvested, washed with fluorescence-activated cell sorting (FACS) buffer, and stained with antibodies for 30 minutes at room temperature, and flow cytometric analysis was performed using BD Celesta. Multicolor staining was performed as described earlier.[19] Antibodies are listed in supplemental Table 1B.

Quantitative RT-PCR

Real-time quantitative reverse transcription polymerase chain reaction (QRT-PCR) was performed as previously described.[30] Primers are listed in supplemental Table 2.

Chromatin immunoprecipitation assay (ChIP)

ChIP assay was carried out with Simple ChIP Enzymatic Chromatin IP Kit (Cell Signaling Technology) as described earlier.[30,31] ChIP primers are shown in supplemental Table 3.

Transient transfection and lentiviral transduction

Control small interfering RNA (Horizon Discovery, CO) and CCR1 siRNAs (Sigma-Aldrich, MO) were transfected into THP1 cells for 48 to 72 hours using Lipofectamine RNAiMAX Transfection Reagent (13778150; Invitrogen) and Opti-MEM Reduced Serum Medium (31985070; Gibco) according to the manufacturer's protocols. Human shRNA for IL-10Rα (Sigma-Aldrich, MO) was used to abrogate the expression of IL-10Rα in MCL. The IL-10Rα shRNA lentiviruses were packaged by cotransfecting shRNA plasmids with packaging constructs in 293T cells. The cells were incubated with lentiviruses mixed with 8 μg/mL polybrene, and the stable expression of shIL-10 Rα was established by puromycin (1 mg/mL) selection.

Western blotting

Western blotting was performed as described earlier.[30] Antibody detection was performed with an enhanced chemiluminescence reaction and analyzed by an LI-COR system (Bio-Rad).

Bioinformatics analysis

Gene expression levels were extracted from the Oncomine database using the search toolbox for "CCR1 or IL-10R" and "MCL". From the given mRNA microarray data, Affymetrix Human Genome U95A-Av2 Array was selected.[32] The reporter IDs for CCR1, IL-10Rα, and IL-10Rβ mRNA expression were 1128_s_at, 35659_at, and 33228_g_at, respectively. CCR1 expression (single-cell sequencing) data were also obtained from the publicly available program "The Human Protein Atlas."

RNA-sequencing

Total RNA was prepared using the RNeasy kit (Qiagen). Library preparation sequencing and primary analysis were performed using GENEWIZ, a biotechnology company (NJ) using the Illumina Hi-sequencing sequencing system. The sequencing data are presented in supplemental Table 5.

Animals and in vivo experiments

All mouse experiments were conducted following the protocols approved by the Institutional Animal Care and Use Committees (IACUC) of George Washington University. Wild-type (WT) immunocompetent mice (C57BL/6J), CCR1 or IL-10 knock-out (KO) mice (C57BL/6NJ) were bought from Jackson Laboratory (Bar Harbor, ME). (A) Syngeneic lymphoma model: 6-week-old male C57BL/6J mice were subcutaneously inoculated with murine lymphoma cell line FC-muMCL1 in both flanks. FC-muMCL1 cells were mixed with an equal amount of growth factor reduced matrigel (Corning, NY). Animals were divided into following 3 groups (n = 6 per group): control, early treatment, or late treatment. For the early treatment group (day 1 after cell inoculation), mice were treated with 50 mg/kg of CCR1 inhibitor (BX-471) the day after injection. For the late treatment group (7 days after cell inoculation), mice were treated with 50mg/kg of BX-471 after the established tumors (volume ~100-150 mm^3) were observed. BX-471 injections were given on alternate days for 2 weeks or until the control tumors reached the predefined end point. Tumor size and mice weight were measured at the indicated times as shown in the figures and figure legends. (B) *CCR1 KO* mice and WT mice were used to extract peritoneal macrophage (PEM) in vivo. For PEM generation in vivo, the mice (n = 5) were peritoneally injected with a 3% brewer thioglycolate medium for 3 to 4 days. Peritoneal cells were obtained after 3 to 4 days by rinsing the peritoneal cavity with cold PBS.

Statistics

Statistical analysis was performed using one-way ANOVA or t test using GraphPad Prism 7.0 software. Unless indicated otherwise, data are expressed as mean ± standard deviation. All the figures have clear labeling, and the error bars with the *P*-values are derived from appropriate statistical tests. $P < .05$ was considered significant. Moreover, each bar is coded with distinct graphic patterns in any given data set for clarity.

Results

Tumor-derived CCL3 plays a key role in monocyte/macrophage migration in MCL models

Macrophage accumulation in most tumors is mainly monocyte derived. We assessed in vitro trafficking of the human or murine

Figure 1. Role of tumor-CCL3 in monocyte migration. (A) $CD14^+$ Mo was incubated with normal plasma (n = 3) or plasma of patients with MCL (n = 5) and migration was assessed using chemotaxis assay (*$P < .05$). (B) Immunofluorescent staining was performed on the syngeneic mouse tumor–bearing FC-muMCL1 murine MCL cell line using the Ly6C (red) antibody. Data were repeated in 3 mouse tumors, and representative data are shown along with quantification. (C) RNA sequencing data demonstrating chemokines (CCL2, CCL3, and CCL4) expression in the MCL cell lines (n = 3) and normal $CD19^+$ B-cells (n = 2). (D) The secretion level of CCL3 in normal $CD19^+$ B cells and MCL cell lines were measured by ELISA. ***$P < .001$ vs CD19. (E) CCL3 was measured in the plasma collected from patients with MCL (n = 5) and normal control participants (n = 3) by ELISA. (F-H) CM collected from MCL cell lines (Mino, Granta, and JVM2) were used to attract THP1-Mo using a chemotaxis assay. An isotype control or 0.5 μg/mL neutralizing anti-CCL2, anti-CCL3, anti-CCL4, or anti-CCL5 antibodies was included in the assay. The data presented are representative of 3 independent experiments. **$P < .01$ vs media alone. (I-J) Mino or Granta CM (I) or plasma of patients with MCL (J) (n = 5) was used to attracting $CD14^+$ Mo in the chemotaxis assay. The data presented are representative of 3 independent experiments. *$P < .05$; **$P < .01$.

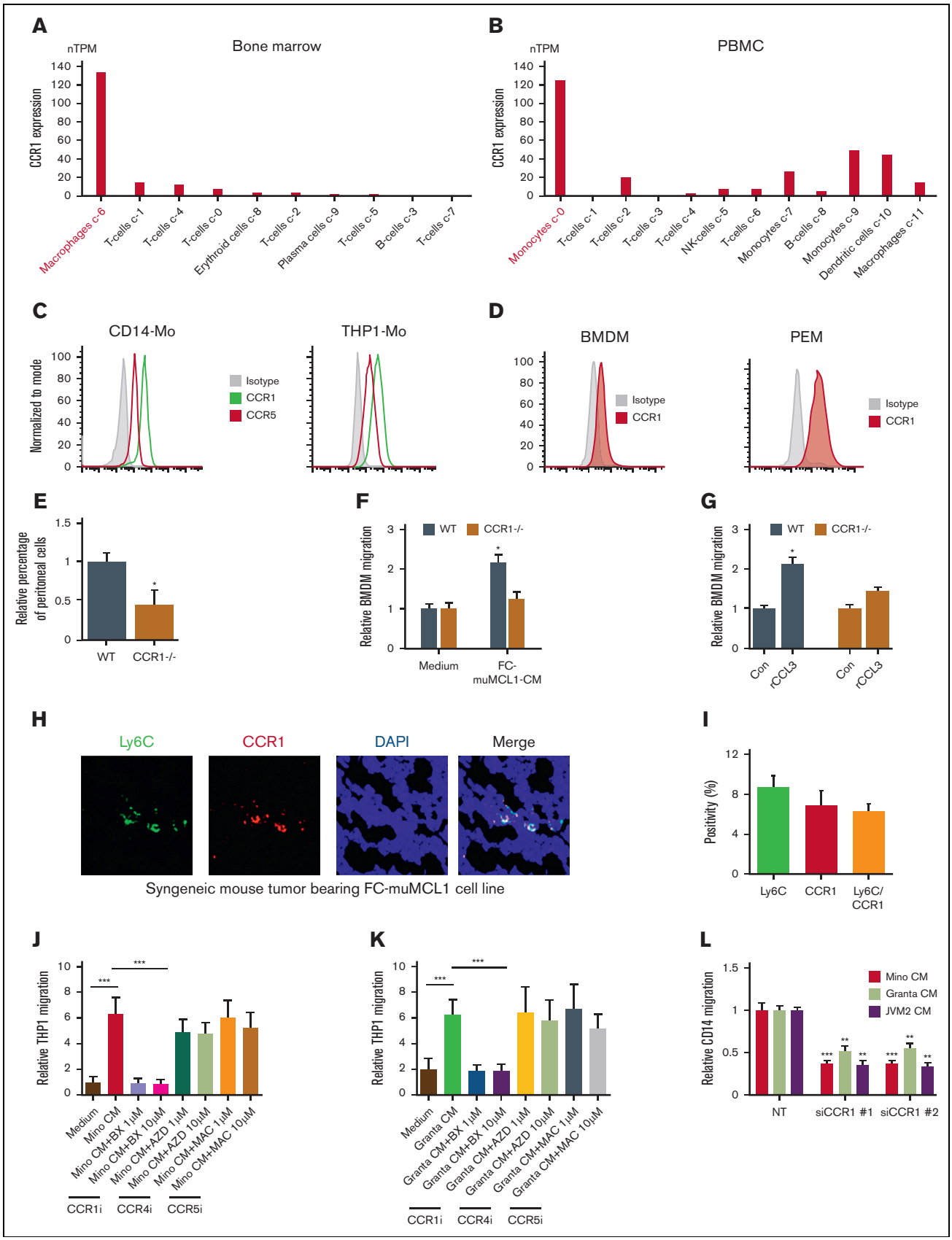
A
Bone marrow
nTPM
CCR1 expression
Macrophages c-6
T-cells c-1
T-cells c-4
T-cells c-0
Erythroid cells c-8
T-cells c-2
Plasma cells c-9
T-cells c-5
B-cells c-3
T-cells c-7
B
PBMC
nTPM
CCR1 expression
Monocytes c-0
T-cells c-1
T-cells c-2
T-cells c-3
T-cells c-4
NK-cells c-5
T-cells c-6
Monocytes c-7
B-cells c-8
Monocytes c-9
Dendritic cells c-10
Macrophages c-11
C
CD14-Mo
THP1-Mo
Normalized to mode
Isotype
CCR1
CCR5
D
BMDM
PEM
Isotype
CCR1
E
Relative percentage of peritoneal cells
WT
CCR1-/-
F
Relative BMDM migration
WT
CCR1-/-
Medium
FC-muMCL1-CM
G
Relative BMDM migration
WT
CCR1-/-
Con
rCCL3
Con
rCCL3
H
Ly6C
CCR1
DAPI
Merge
Syngeneic mouse tumor bearing FC-muMCL1 cell line
I
Positivity (%)
Ly6C
CCR1
Ly6C/ CCR1
J
Relative THP1 migration
Medium
Mino CM
Mino CM+BX 1μM
Mino CM+BX 10μM
Mino CM+AZD 1μM
Mino CM+AZD 10μM
Mino CM+MAC 1μM
Mino CM+MAC 10μM
CCR1i
CCR4i
CCR5i
K
Relative THP1 migration
Medium
Granta CM
Granta CM+BX 1μM
Granta CM+BX 10μM
Granta CM+AZD 1μM
Granta CM+AZD 10μM
Granta CM+MAC 1μM
Granta CM+MAC 10μM
CCR1i
CCR4i
CCR5i
L
Relative CD14 migration
Mino CM
Granta CM
JVM2 CM
NT
siCCR1 #1
siCCR1 #2

Figure 2.

Mo and macrophages (MΦ) by performing a chemotaxis assay using CM collected from MCL cell lines and plasma from patients with MCL. Data demonstrate that Mo/MΦ significantly migrated towards MCL-CM or MCL-plasma compared with the control (Figure 1A; supplemental Figures 1A-F). Next, we analyzed the infiltration of Mo in syngeneic mice bearing murine MCL cell line FC-muMCL1 using antibodies against Ly6G (granulocytic marker) and Ly6C (monocytic/macrophage marker). Increased infiltration of $Ly6C^+$, but not $Ly6G^+$, was observed in the mouse tumors bearing MCL (Figure 1B).

Next, we sought to identify the key chemokine produced by MCL cells that is responsible for the Mo/MΦ migration. We have shown earlier that several chemokines including CCL3 (MIP-1α) or CCL4 (MIP-1β) were significantly elevated in the serum of untreated patients with MCL compared with normal control participants.[33] RNA-sequencing data performed in the MCL cell lines (Mino, JVM2, and Granta) and normal B cells ($CD19^+$) confirmed an increased expression of CCL3 in MCL cell lines than in normal B cells (Figure 1C). We also compared the CCL3 mRNA expression of the monocytes (THP1 and U937 cell lines) and MCL cells (Mino and JVM2) and found that monocytes express lower mRNA levels of CCL3 as compared with the MCL cells (supplemental Figure 1G). Furthermore, we observed significantly higher ($P < .01$) secretion of CCL3 protein in MCL cell line supernatants and in plasma from patients with MCL compared with normal control participants (Figure 1D-E). Exogenous addition of recombinant CCL3 (rCCL3) increased the migration of the THP1- and U937-Mo in a dose-dependent manner confirming the chemoattractant ability of chemokine CCL3 (supplemental Figure 1H).

The effects of chemokines on the chemotaxis of THP1-Mo and $CD14^+$ Mo were then assessed by specific neutralizing antibodies against CCL2, CCL4, CCL5, and CCL3, along with isotype control. As shown in Figure 1F-H, the neutralization of CCL3, rather than that of CCL2, CCL4, or CCL5, significantly ($P < .01$) abrogated the THP1-Mo migration. The combination of all 4 neutralizing antibodies (CCL2, CCL3, CCL4, and CCL5) was comparable to the CCL3 antibody alone in suppressing Mo migration, which indicates the prominent effect of CCL3 on Mo-migration. Furthermore, the CCL3 neutralizing antibody was able to inhibit the migration of human $CD14^+$ Mo (freshly isolated from healthy donors) toward CM collected from Mino or Granta (Figure 1I). This was further proved in plasma collected from the primary patients with MCL (Figure 1J). Overall, these results suggest that lymphoma cells–derived CCL3 exhibits the essential function of monocyte migration/infiltration.

CCR1 is highly expressed in monocytes/macrophages and is required for their migration

Immune cells including MΦ are well known to express chemokine receptors. We obtained the single-cell sequencing data of CCL3 cognate receptor CCR1 on immune cells from the publicly available data set source "the Human Protein Atlas." Results demonstrate that macrophages expressed high CCR1 mRNA compared with other immune cells in the BM. Similarly, monocytes expressed high CCR1 mRNA in the PBMCs compared with other immune cells (Figure 2A-B). Our flow cytometry data confirmed high CCR1 expression on $CD14^+$ Mo, THP1-Mo, and murine MΦ obtained from BM and PEM in immunocompetent C57BL/6 mice (Figure 2C-D). Interestingly, CCR1 levels were found to be nil to low on the human MCL (Mino, JVM2, and Granta) or murine MCL (FC-muMCL1) cell lines (supplemental Figures 2A-B). Bioinformatic analysis using the Oncomine tool confirmed lower mRNA expression of CCR1 on MCL tumors as compared with normal B cells and other B-cell lymphomas (supplemental Figure 2C), supporting our in vitro findings.

To confirm the role of CCR1 in MΦ or Mo migration in vivo, we generated peritoneal macrophages (PEM) and BMDM from the CCR1 KO (*CCR1-/-*) and WT mice as described in the method section. There was no obvious morphological difference seen between the PEM or BMDM from both groups (supplemental Figure 3A). Analyzing in vivo MΦ migration in response to intraperitoneal administration of thioglycolate revealed that significantly ($P < .05$) fewer thioglycolate-elicited cells were recovered in *CCR1-/-* mice than in WT mice. Moreover, a decrease in the $CD11b^+/F4/80^+$ MΦ population in the *CCR1-/-* PEM compared with WT PEM was noted as well (Figure 2E; supplemental Figure 3B). We did not observe noticeable infiltration of the $CD11b^+/F4/80^-$ population (myeloid/neutrophils) in both groups (data not shown). In vitro chemotaxis assay showed that BMDM from *CCR1-/-* mice exhibited impaired migration to FC-muMCL1-CM or exogenous CCL3 as compared with WT BMDM, suggesting the importance of CCR1 in MΦ/Mo migration (Figure 2F-G). Furthermore, immunofluorescence performed on the syngeneic mouse tumors bearing murine MCL cell line FC-muMCL1 tumor indicated that the majority of the Ly-$6C^+$ (monocytic) cells coexpressed CCR1 (Figure 2H-I).

Given the above data indicating a key role of CCR1 in Mo/MΦ migration toward MCL, we tested whether interfering with CCR1 would inhibit migration and be potentially therapeutic. Pretreatment with the CCR1-specific inhibitor BX-471 significantly ($P < .001$) impaired the in vitro migration ability of THP1 Mo to Mino and

Figure 2. CCR1 is highly expressed in monocyte/macrophages and facilitates migration. (A-B) The bioinformatics analysis demonstrates CCR1 expression on various immune cells in the BM and PBMC. (C-D) The expression of CCR1 or CCR5 in human-Mo (C) and murine-macrophages (D) was measured using flow cytometry using specific antibodies. (E) The number of peritoneal cells collected from WT and *CCR1-/-* mice after thioglycolate in vivo treatment in the peritoneal cavity (n = 5). (F) BMDM from WT or *CCR1-/-* C57/BL/6NJ mice (n = 5) were incubated with CM collected from FC-muMCL1, and the migration was assessed using chemotaxis assay. (G) BMDM from WT or *CCR1-/-* mice (n=5) were incubated with 100 ng/mL rCCL3 in vitro, and the migration was assessed using a chemotaxis assay. The data presented are representative of 3 independent experiments (*$P < .05$). (H-I) Immunofluorescent staining was performed on the syngeneic mouse tumor–bearing lymphoma using Ly6C (green) and CCR1 (red) antibodies. The experiment was performed on 3 mouse tumors and representative data are shown along with quantification. Nuclei were stained with DAPI (blue). (J-K) Mino (J) or Granta (K) CM treated with vehicle or indicated concentrations of CCR1 antagonist (BX-471), CCR4 antagonist (AZD2089), or CCR5 antagonist (Maraviroc) for 48 hours were used to attract THP1-Mo in a chemotaxis assay. (L) MCL (Mino, Granta, or JVM2) CM was used to attract $CD14^+$ Mo transfected with CCR1 or control siRNA. The data presented are representative of 3 independent experiments (**$P < .01$; ***$P < .001$).

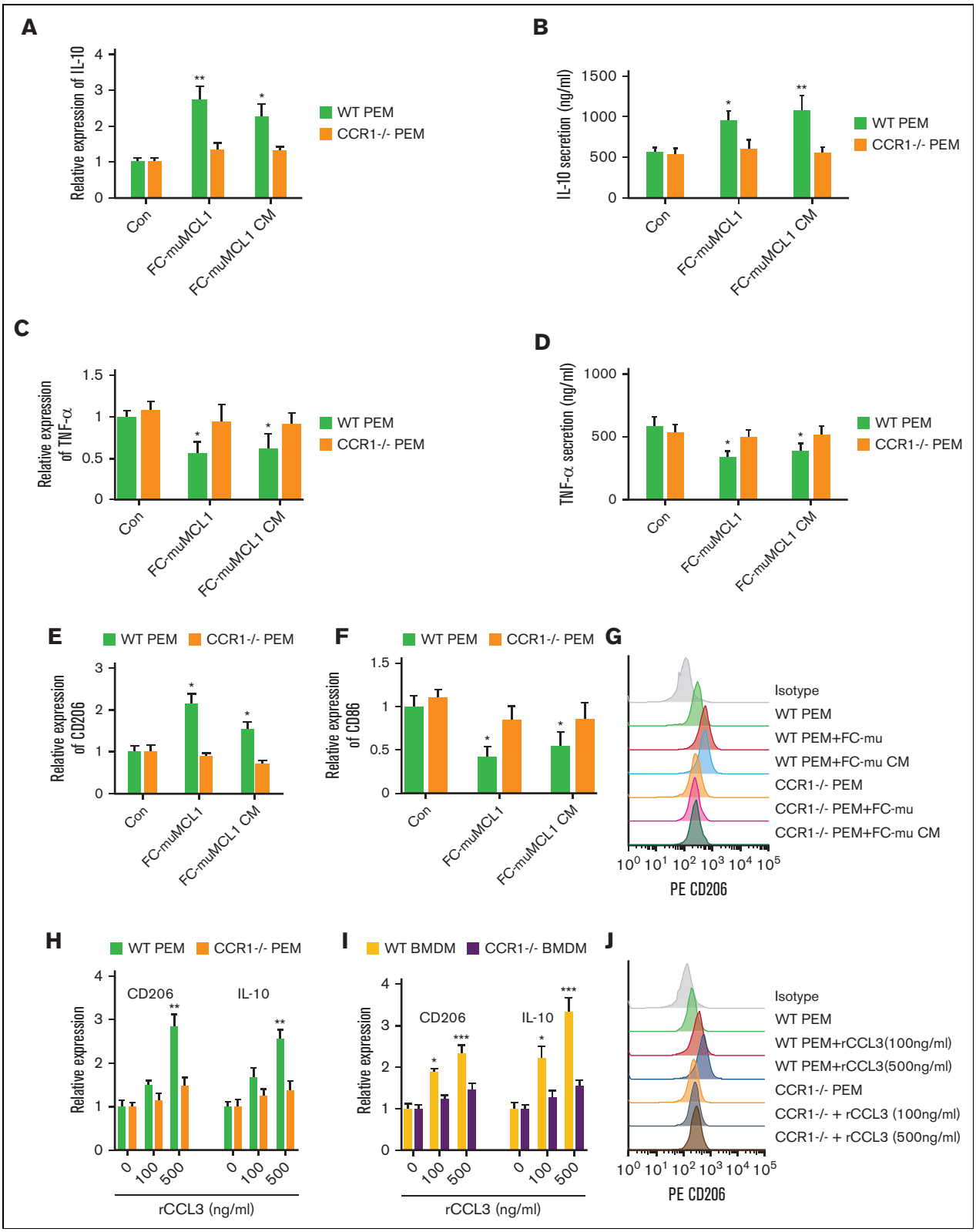

Figure 3. CCL3-CCR1 axis-mediated macrophage polarization. (A-D) WT or *CCR1-/-* PEM (n = 3) were cocultured with FC-muMCL1 or incubated with CM collected from FC-muMCL1 for 48 hours, and IL-10 mRNA (A), IL-10 secretion (B), TNF-a mRNA expression (C), and TNF-a secretion (D) in PEM was assessed using qRT-PCR and ELISA, respectively. (E-G) WT or *CCR1-/-* PEM (n = 3) were cocultured with FC-muMCL1 or incubated with CM collected from FC-muMCL1 for 48 hours; and mRNA levels of CD206 and CD86, and CD206 surface expression were assessed using qRT-PCR and flow cytometry, respectively. (H-I) The mRNA level of CD206 and IL-10 in response to

Granta CM, whereas minimal effects of CCR4 inhibitor AZD2089 and CCR5 inhibitor maraviroc were seen on THP1-Mo migration (Figure 2J-K). Similar results were obtained when CCR1 was depleted using 2 different siRNAs, which significantly ($P < .001$) decreased $CD14^+$ Mo migration to the Mino, Granta, and JVM2 CM (Figure 2L; supplemental Figure 3C). These results implied that inhibition of CCR1 may be a viable therapeutic strategy to target TAMs.

Tumor-CCL3 programs macrophage polarization in CCR1-dependent manner

To identify the role of the CCL3-CCR1 axis in macrophage programming, first, we cocultured the PEM collected from *CCR1-/-* or WT mice with FC-muMCL1 and assessed the expression of M1 and M2 macrophage cytokines and markers. Results showed that FC-muMCL1 direct coculture or CM treatment significantly increased the IL-10 mRNA expression and secretion in the PEM from WT mice, which was not observed in the PEM from *CCR1-/-* mice (Figure 3A-B). In contrast, a significant decrease in TNFα expression and secretion was seen in the WT-PEM compared with PEM from *CCR1-/-* mice (Figure 3C-D). We further examined the expression of the M1 and M2 markers in PEM from WT and *CCR1-/-* upon direct coculture or CM treatment. Under these conditions, M2 marker CD206 was increased and M1 marker CD86 was decreased as assessed by QRT-PCR (Figure 3E-F). Next, we analyzed the surface expression of M2 marker CD206 using flow cytometry in a similar setting. We observed increased surface expression of CD206 when WT PEM cocultured or CM treated with FC-muMCL1. In contrast, no obvious effect was observed in the *CCR1-/-* PEM under similar conditions (Figure 3G).

To further investigate the contribution of CCR1 in CCL3-mediated MΦ polarization, we treated the *CCR1-/-* BMDM or PEM with exogenous CCL3 and assessed the expression of M1 and M2 markers. A dose-dependent increase in the expression of M2 markers CD206 and IL-10 were seen in the WT PEM and BMDM in response to CCL3, although the level of CD206 and IL-10 remained unaltered in *CCR1-/-* PEM and BMDM (Figure 3H-I). Contrary to this, a dose-dependent decrease in the expression of M1 marker CD86 was seen in the WT BMDM or PEM in response to rCCL3, although CD86 levels remained unaltered in *CCR1-/-* PEM or *CCR1-/-* BMDM as compared with the basal levels (supplemental Figures 4A-B). We confirmed that CD206 surface expression was also increased in WT PEM in response to exogenous CCL3, although CD206 expression remained unchanged in *CCR1-/-* PEM in response to CCL3 (Figure 3J). Altogether these data suggest that CCR1 is required in CCL3-mediated macrophage polarization in MCL models.

CCR1 inhibitor reverses the effect of CCL3-mediated macrophage programming

Next, we intended to reverse the CCL3-mediated effects on MΦ polarization by using CCR1-specific inhibitor BX-471 and CCL3-neutralizing antibody using a 2D coculture system. Mino cells cocultured with THP1-MΦ or U937-MΦ were treated with BX-471 (1 μM) or CCL3 neutralizing antibody (0.5 μg/mL), and the expression of the M2-MΦ markers CD206, IL-10, or M1 marker CD86 was assessed. Coculturing Mino with U937- or THP1-MΦ significantly increased the CD206 and IL-10 expression, which was severely inhibited in response to BX-471 or CCL3-neutralizing antibody (Figure 4A). In contrast, coculturing Mino with THP1- or U937-MΦ reduced the M1 marker CD86, althogh targeting CCR1 or CCL3 restored CD86 expression in THP1- or U937-MΦ cells close to the basal levels in a vitro co-culture system with Mino (Figure 4B). Next, we sought to confirm the cell line findings in the primary cells from patients with MCL and assessed the effect of M2 and M1 markers by coculturing with $CD14^+$ Mo treated with CCL3 antibody and CCR1 inhibitor. We observed that MCL-mediated upregulation of M2 marker CD206 and IL-10 was restored in the CCR1 or CCL3 targeted settings. We observed that the MCL cells reduced the M1 marker CD86 slightly, which was recovered by CCR1 or CCL3 targeting (Figure 4C). Next, we treated THP1-MΦ with CM from Mino, or JVM2 with or without BX-471, and IL-10 secretion was analyzed by ELISA. The blockade of CCR1 prevented the secretion of IL-10 induced by MCL cells (Figure 4D).

We recently showed that MCL cells polarize intratumoral macrophages to M2-phenotype by regulating immunosuppressive IL-10.[19] We confirmed the coexpression of IL-10 with CD206 in syngeneic mouse tumors bearing FC-muMCL1 using immunofluorescence (Figure 4E). We explored the impact of IL-10 deletion on MΦ-polarization, using BMDM from WT and *IL-10-/-* mice. BMDM from *IL-10-/-* mice exhibited a lower expression of M2 marker CD206 than WT-BMDM. Furthermore, the addition of exogenous recombinant IL-10 rescued the M2-phenotype in *IL-10-/-* BMDM by significantly ($P < .01$) increasing the CD206 expression (Figure 4F). Increased M1 markers CD86 and MHC II were observed in the *IL-10-/-* BMDM compared with the WT-BMDM, and the addition of exogenous IL-10 decreased the M1 markers (Figure 4G). Overall, these results shed light on the unique role of the CCL3-CCR1 axis in MΦ programming.

Macrophage-derived IL-10 increased tumor-derived CCL3 via IL-10Rα

We sought to determine if increased IL-10 by MΦ during polarization provides feedback to tumor-CCL3 as part of a continuous circuit for monocyte recruitment. First, we measured CCL3 expression and secretion in MCL cell lines, Mino, JVM2, and Granta after stimulating with recombinant IL-10. Treatment with IL-10 significantly ($P < .05$) and markedly enhanced CCL3 expression and secretion in a dose-dependent manner in all the tested MCL cell lines (Figure 5A-B). Next, we verified the role of IL-10 in CCL3 regulation using BMDM from *IL-10* KO mice and cocultured with murine MCL cell line FC-muMCL1. As shown in Figure 5C, the expression of CCL3 on FC-muMCL1 was significantly upregulated when treated with WT-BMDM CM, whereas the expression of CCL3 remained unaltered in response to *IL-10-/-* BMDM CM.

Figure 3 (continued) various concentrations of CCL3 was assessed in WT (n = 3) or *CCR1-/-* (n = 3) PEM (H) or WT and *CCR1-/-* BMDM (I) using qRT-PCR. (J) WT or *CCR1-/-* PEM (n = 3) were incubated with exogenous 100 ng/mL or 500 ng/mL CCL3 and CD206 expression was analyzed using flow cytometry. Data presented are representative of 3 independent experiments until or otherwise stated (*$P < .05$; **$P < .01$).

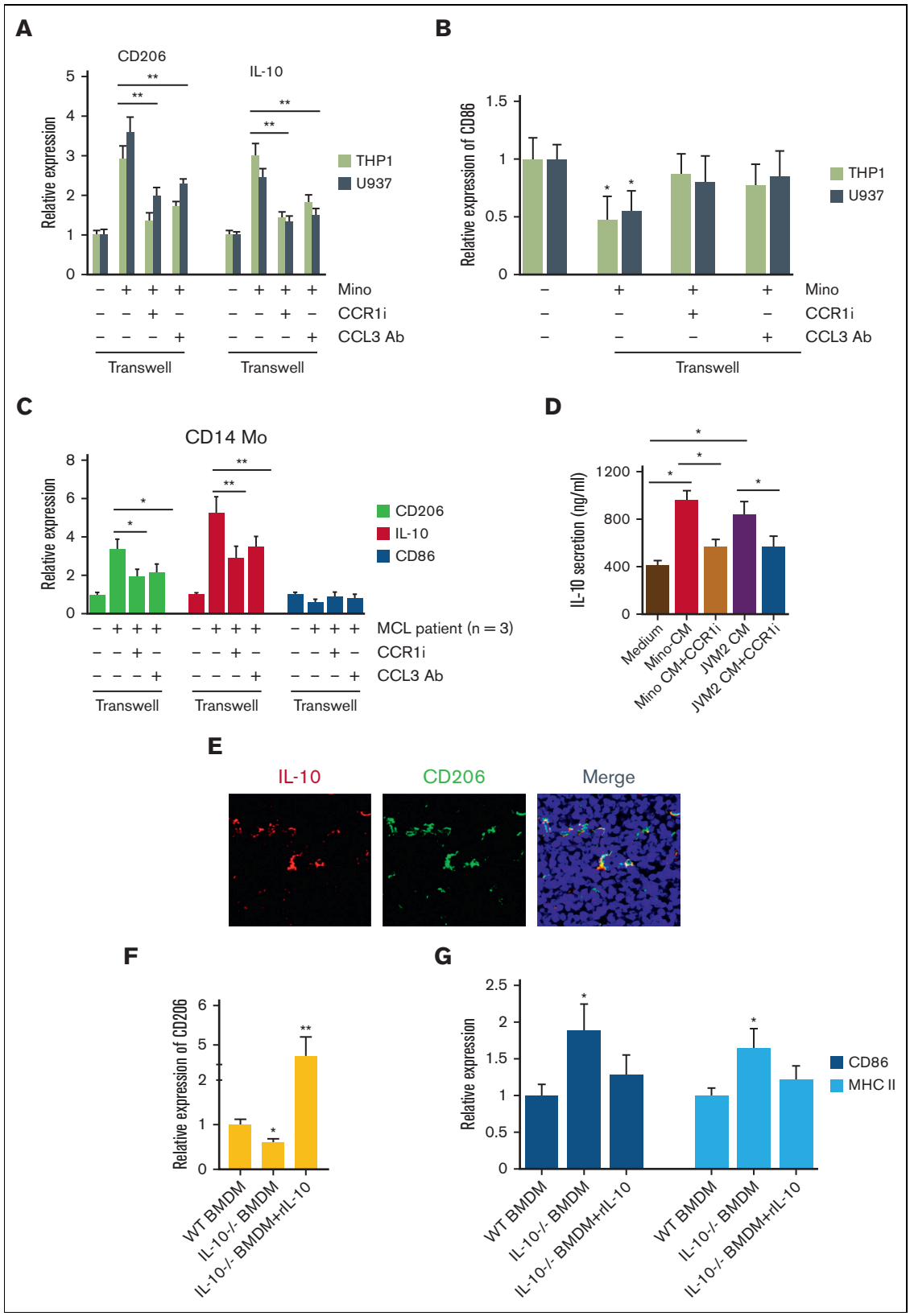

Figure 4. Effect of inhibition of CCL3-CCR1 axis on macrophage programming. (A-B) THP1- and U937-MΦ were cocultured with Mino cells and treated with or without 1μM CCR1 inhibitor or 0.5 μg/mL of CCL3 neutralizing antibody for 48 hours and expression of CD206 and IL-10 (A) or CD86 (B) mRNA was assessed. (C) Cells from the patients with MCL were cocultured with $CD14^+$ Mo and treated with or without 1μM CCR1 inhibitor or 0.5 μg/mL of CCL3 neutralizing antibody and mRNA expression of

Interestingly, adding back IL-10 to *IL-10-/-* BMDM CM could rescue CCL3 expression, suggesting the expression of CCL3 on MCL for the responsiveness of IL-10.

IL-10 exerts its function via IL-10Rα and IL-10Rβ,[34] and bioinformatics (Oncomine database) data demonstrated significantly ($P < .01$) higher expression of IL-10Rα than IL-10Rβ in MCL tumors as compared with normal controls (supplemental Figures 5A-B). Monocytes and monocytes-derived macrophages have been shown to express IL-10Rα.[35] We identified low expression of IL-10Rα on the $CD14^+$ Mo and THP1-Mo (supplemental Figure 5C). We further confirmed the in vivo coexpression of IL-10Rα and $CD19^+$ B cells using immunofluorescence in syngeneic MCL mouse tumors bearing FC-muMCL1 (Figure 5D). The responsiveness of IL-10Rα and IL-10Rβ toward IL-10 was investigated in MCL cell lines (Mino and JVM2) and in cells of patients with MCL. MCL cells cultured with rIL-10 were analyzed for changes in the expression of IL-10Rα and IL-10Rβ. As presented in Figure 5E, IL-10 concentration upregulated the expression of IL-10Rα, but not IL-10Rβ, in a dose-dependent manner (Figure 5E; supplemental Figure 5D).

To further confirm the role of IL-10/IL-10Rα in regulating tumor CCL3, we inhibited IL-10Rα signaling in MCL cells using IL-10Rα shRNA. When THP1-MΦ was incubated with Mino and JVM2 transfected with IL-10Rα or control (scrambled) shRNA, CCL3 expression and secretion levels were significantly diminished in IL-10Rα knock-down MCL cells as compared with control cells (Figure 5F-G). Furthermore, migration of THP1 Mo significantly increased in response to the CM from rIL-10 treated MCL cells, which was abolished either by treatment of CCR1 inhibitor or CCL3 Ab (Figure 5H). These results suggested a paracrine feedback loop between IL-10 and CCL3.

IL-10 regulates CCL3 expression via STAT1 signaling

To identify the connecting link between CCL3 and IL-10, we analyzed potential transcription factor binding sites enriched on the CCL3 promoter region and identified an abundance of binding motifs for STAT1 and STAT3 transcription factors (supplemental Figures 6A-B). To determine whether STAT1 or STAT3 played a role in CCL3 regulation, chromatin immunoprecipitation (ChIP) assays were conducted using immunoprecipitation by STAT1 or STAT3 antibodies. It was observed that STAT1, but not STAT3, was highly enriched in the CCL3 promoter region. Further ChIP analysis demonstrated that IL-10 treatment increased the STAT1 binding to the CCL3 promoter region, suggesting that IL-10 might regulate CCL3 expression via STAT1 (Figure 6A-B). CCL3 secretion induced by IL-10 was significantly ($P < .01$) reduced when combined with a STAT1-specific inhibitor (Figure 6C).

Next, to investigate whether macrophage-IL-10 contributed to CCL3-mediated STAT1 signaling in MCL, FC-muMCL1 cells were cocultured with WT or *IL-10-/-* BMDM, or treated with CM collected from BMDM, and pSTAT1 expression was assessed. *IL-10-/-* BMDM CM or coculture resulted in decreased pSTAT1 compared with the coculture or CM treatment of WT BMDM in FC-muMCL1 cells. Furthermore, the pSTAT1 level in MCL was upregulated when cocultured with THP1-MΦ, which was abolished by the CCR1 inhibitor (Figure 6D-E). These data altogether suggest that CCL3/CCR1 axis is responsible for upregulating IL-10, which eventually results in STAT1 activation in MCL. These data establish an association linking IL-10 and the CCL3/CCR1 axis in playing an important role in the MCL tumor-microenvironment.

Moreover, the increase in pSTAT1 level in MCL cell lines mediated by THP1-MΦ CM was almost entirely abolished when IL-10Rα was knocked down using shRNA**.** Enrichment of STAT1 binding at CCL3 promoter region mediated by THP1-MΦ CM was significantly decreased in IL-10Rα knock-down MCL cells compared with control cells (Figure 6F-G). These results suggested that IL-10/IL-10Rα regulates CCL3 in lymphoma cells via STAT1 signaling.

CCR1 inhibition is protective against MCL in vivo using the syngeneic model

To explore the potential pathogenic role of CCR1 in lymphomagenesis, we injected the murine MCL cell line FC-muMCL1 into the syngeneic C57BL/6 model (n = 6 mice in each group) and grouped it into the following 3 subgroups: (A) cell line alone, (B) starting CCR1 inhibitor (BX-471) injection once visible tumors are formed (around 7 days), and (C) starting BX-471 injection the next day after cell line inoculation. Compared with control mice (Group A), both CCR1 inhibitor–treated groups (B and C) showed significant ($P < .01$) growth inhibition leading to smaller tumor weight and volume at the time of euthanization. In group C, tumors were much smaller as compared with the tumors in group B where CCR1 treatment started once the visible tumors formed (Figure 7A). Moreover, tumor in group C was lower in tumor volume and weight as compared with other groups (Figure 7B-C).

Immunofluorescence analysis showed nil to very low infiltration of the $CD11b/Gr1^+$ (neutrophils) population in the MCL mouse tumors of any group**.** Further analysis showed a significant reduction in the $F4/80^+CD206^+$ M2-TAMs in the CCR1 inhibitor–treated groups as compared with the untreated group (Figure 7D-E). Increased $CD8^+$ T cell infiltration into both the treated groups (compared with the untreated group, although group C showed increased CD8 infiltration in comparison with the group B) was observed (Figure 7F). The percentage changes in the proportion of $CD206^+/F4/80^+$ M2-TAMs and $CD8^+$ T cells in the CCR1 inhibitor–untreated and treated groups are shown in Figure 7G-H. These observations indicate that CCR1 inhibition decreased the CCL3-CCR1 paracrine signaling axis between tumor and macrophages, thus reducing tumor burden.

Figure 4 (continued) CD206, IL-10, and CD86 was evaluated using qRT-PCR. (D) THP1-MΦ were incubated with Mino or JVM2 CM with or without 1μM CCR1 inhibitor BX-471 treatment, and the secretion of IL-10 was assessed using ELISA. (E) Immunofluorescent staining was performed on the syngeneic mouse tumor–bearing FC-muMCL1 cells using IL-10 (red) and CD206 (green) antibodies. Nuclei were stained with DAPI (blue). (F-G) CD206 or CD86 and MHC II expression were assessed in WT (n = 3) or *IL-10-/-* BMDM (n = 3) with or without rIL-10 (100 ng) treatment using qRT-PCR. Data presented are representative of 3 independent experiments unless stated otherwise (*$P <$ .05; **$P < .01$).

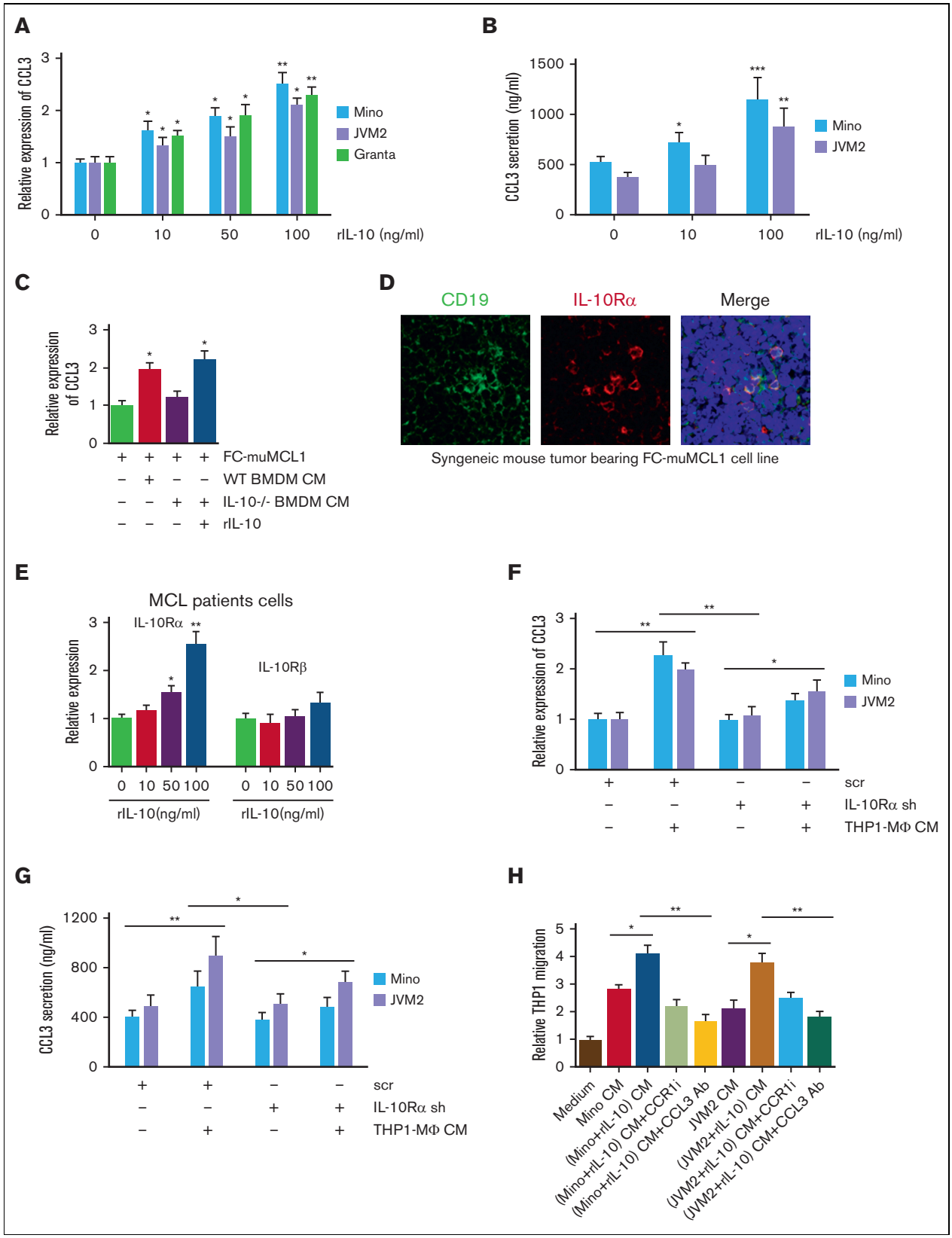

Figure 5. IL-10 regulates tumor-CCL3 expression. (A) Mino, JVM2, and Granta were treated with indicated concentrations of rIL-10 for 48 hours, and CCL3 expression was assessed using qRT-PCR. (B) Mino and JVM2 cells were treated with indicated concentrations of rIL-10 for 48 hours, and secretion of CCL3 was assessed using ELISA. (C) FC-muMCL1 cells were treated with CM collected from WT or *IL-10-/-* BMDM treated with or without rIL-10, and the expression level of CCL3 was assessed using qRT-PCR. (D) Immunofluorescent staining was performed on the syngeneic mouse tumors bearing FC-muMCL1 (n = 3) using CD19 (green) and IL-10Rα (red) antibodies. Nuclei

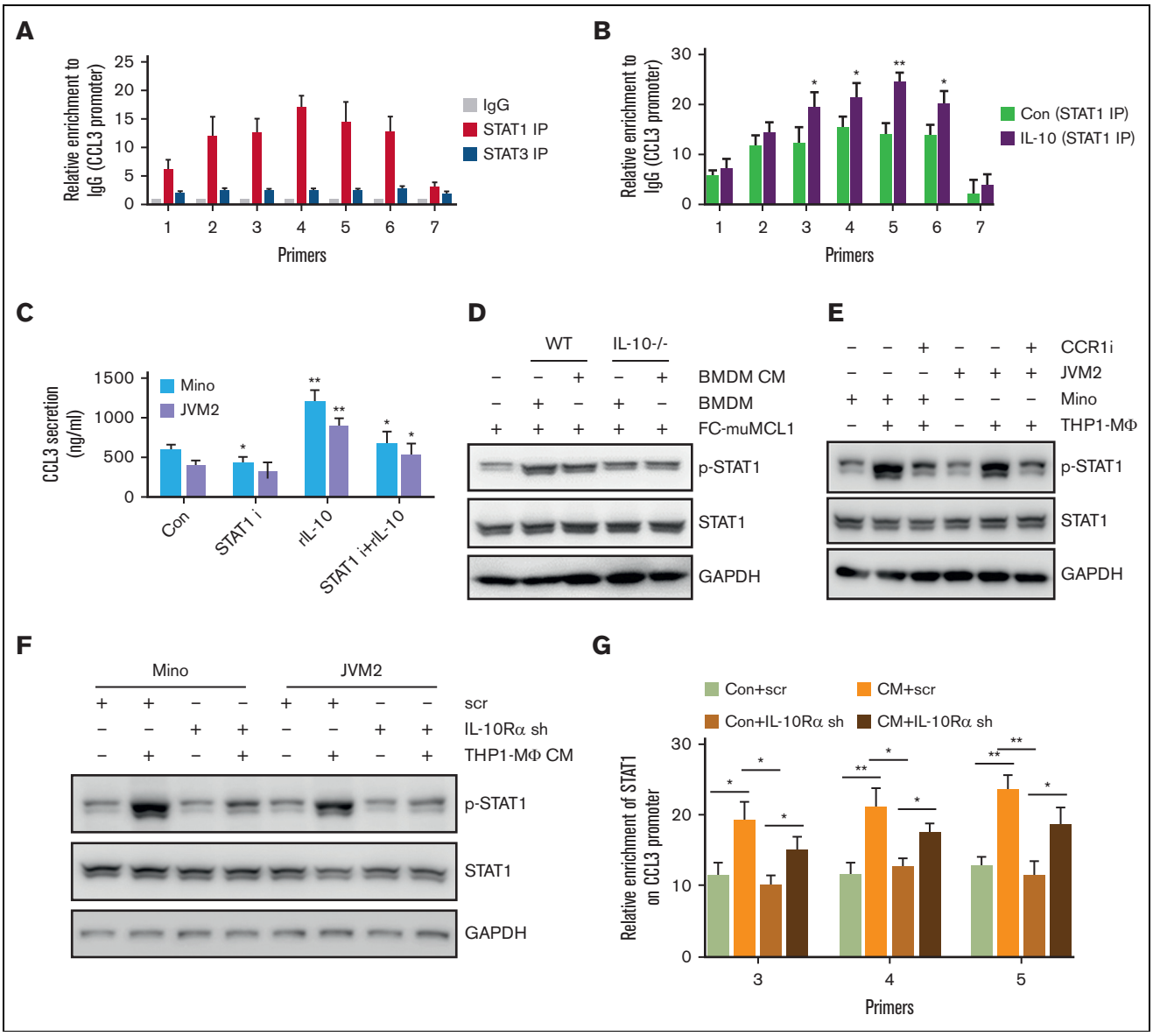

Figure 6. Molecular mechanism of CCL3 regulation by IL-10. (A) ChIP assay was performed to detect enrichment of STAT1 and STAT3 on CCL3 promoters in Mino cells as described in the method section. (B) Mino cells were treated with or without 100 ng/mL rIL-10 for 24 hours, and the enrichment of STAT1 on the CCL3 promoter was detected using ChIP assay. (C) Mino and JVM2 cells were treated with 100ng/ml rIL-10 and/or 1μM STAT1 inhibitor fludarabine for 48h and the secretion of CCL3 was assessed using ELISA. The data presented are representative of 3 independent experiments. *$P < .05$; **$P < .001$. (D) FC-muMCL1 cells were cocultured with BMDM from WT or *IL-10-/-* mice (n = 3) or treated with CM collected from WT and *IL-10-/-* BMDM (n = 3), and the protein level of phospho-STAT1 and STAT1 were assessed using western blotting. (E) Mino or JVM2 cells were cocultured with THP1-MΦ with or without 1μM CCR1 inhibitor BX-471 for 24h, and the protein level of phospho-STAT1 and total STAT1 were assessed using western blotting. The experiment was repeated 3 times with similar results and representative data shown. (F) Mino and JVM2 cells infected with IL-10Rα shRNA or scramble shRNA for 72 hours were incubated with THP1-MΦ CM, and the protein level of phospho-STAT1 and total STAT1 was assessed using western blotting. (G) Mino cells infected with IL-10Rα shRNA or scramble shRNA for 72 hours were incubated with THP1-MΦ CM, and the enrichment of STAT1 on the CCL3 promoter was assessed using ChIP assay. *$P < .05$; **$P < .01$. Data presented are representative of 3 independent experiments unless stated otherwise (*$P < .05$; **$P < .01$; ***$P < .001$).

Figure 5 (continued) were stained with DAPI (blue). A representative experiment is shown. (E) Cells of patients with MCL (n = 5) were treated with indicated concentrations of rIL-10 for 48 hours, and the mRNA level of IL-10Rα and IL-10Rβ were assessed using qRT-PCR. **(**F-G) THP1-MΦ CM was used to treat Mino and JVM2 cells infected with IL-10Rα shRNA or scramble shRNA for 72 hours, and the CCL3 mRNA level (F) and CCL3 secretion (G) were assessed using qRT-PCR and ELISA, respectively. **(**H) THP1 cells were incubated with CM collected from Mino or JVM2 pretreated with or without 100 ng/mL rIL-10 for 48 hours with 1μM CCR1 inhibitor or 0.5 μg/mL anti-CCL3 antibody, and the migration was assessed using chemotaxis assay. Data presented are representative of 3 independent experiments unless stated otherwise (*$P < .05$; **$P < .01$).

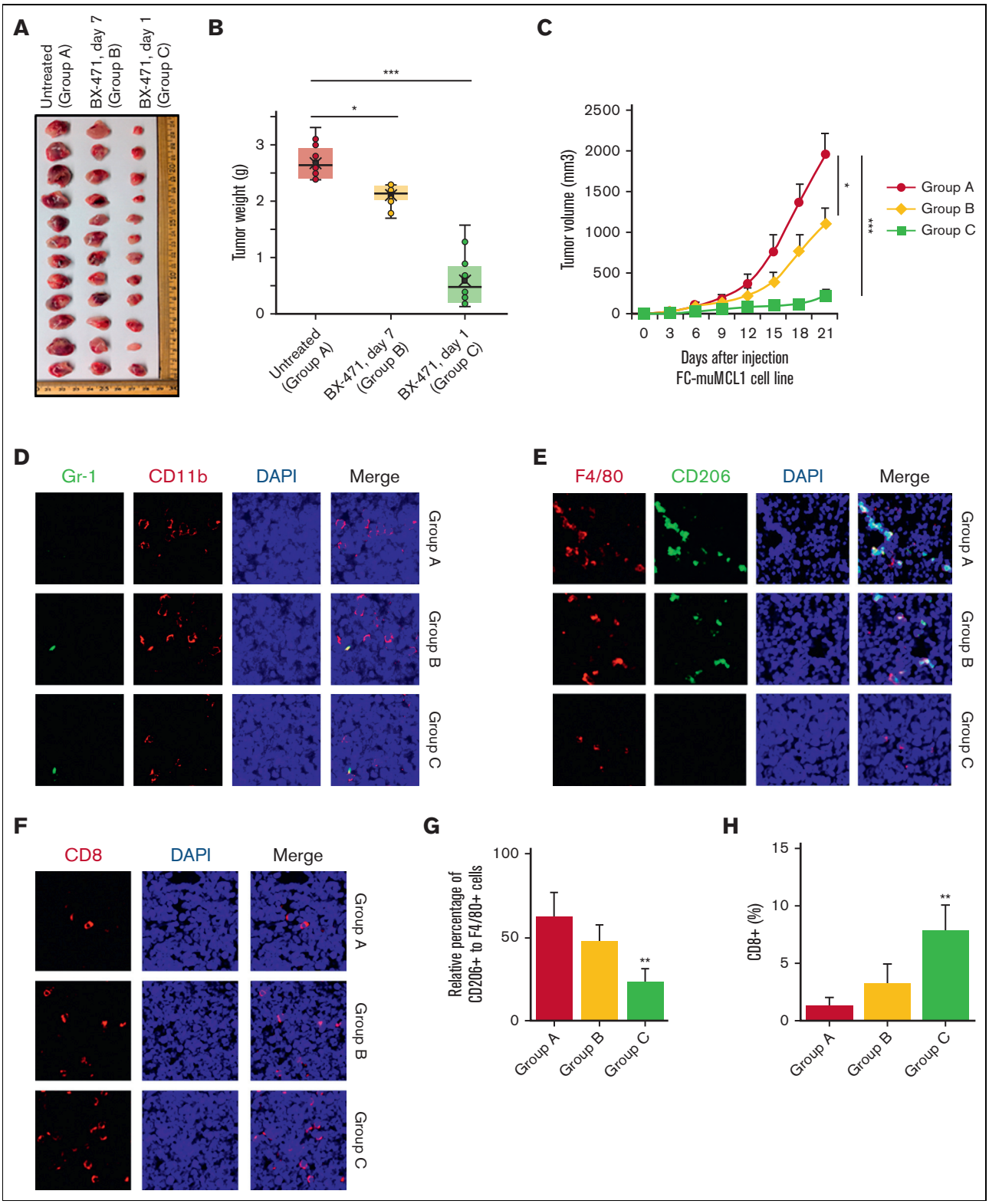

Figure 7. In vivo targeting of CCR1 in a syngeneic lymphoma mouse model. (A) Typical photos of syngeneic mouse tumors bearing murine MCL cell line FC-muMCL1 on day 21 from untreated and BX-471 (50 mg/kg) treated early (day 1) and late (day 7) groups. (B) Tumor weight was assessed among the indicated groups. Treatment with BX-471 decreased tumor weight when measured at day 21 (n = 6 mice) (*$P < .05$; ***$P < .001$) (C). Tumor volume was assessed among the indicated groups. BX-471 treatment decreased tumor volume when measured at day 21 (n = 6 mice) (*$P < .05$; ***$P < .001$). (D) IF was performed on the syngeneic mouse tumors using Gr-1 (green) and CD11b (red) antibodies. The experiment was repeated on 3 mouse tumors. (E) Immunofluorescent staining was performed on the syngeneic mouse tumors using F4/80 (red) and CD206

Discussion

In addition to intrinsic tumor abnormalities, the critical role of immune cells within the tumor microenvironment (TME) in disease progression is emerging. Among the immune cells, TAMs are known to play a critical role in many solid cancers.[13] The dynamic interaction of tumor cells with TAMs in B-cell lymphoma has not been fully elucidated, although some studies described the nurse-like cells as chronic lymphocytic leukemia (CLL) associated with macrophages.[36] Recently, we have reported abundant TAMs within the MCL-niche and their protumor role in MCL tumorigenesis using an in vivo syngeneic MCL model.[19] Our study is consistent with the study by Pham et al describing the involvement of TAMs in vitro during the development of MCL cell line PF-1.[18] A knowledge gap exists in defining the unique paracrine cross talk between tumor cells and TAMs in B-cell lymphoma in general, and MCL in particular, as this is not well established yet. This work, using in vitro and in vivo approaches including an immunocompetent MCL mouse model and patient-derived materials, sheds light on how the tumor cells and TAMs within TME respond by the hyperactivation of a CCL3-IL-10 paracrine axis for macrophage polarization and tumor progression.

Our preliminary experiments demonstrated the migration of $CD14^+$ monocytes and bone marrow-derived macrophage/peritoneal macrophages to MCL tumors suggesting that monocytes/macrophages are directly attracted by key soluble factors produced by malignant B cells. This led us to investigate the key factor(s) secreted by MCL cells which directly recruit monocytes to MCL-TME. Chemokines are known to recruit and activate subsets of leukocytes.[21] Chemokines such as CCL2 (MCP-1) play a critical role in monocyte migration during inflammation.[37] However, we found no evidence that CCL2, CCL4, or CCL5, were involved in our MCL models. In contrast, CCL3 produced by those MCL lines was capable of stimulating monocyte/macrophage migration, and CCL3 neutralization almost completely inhibited this migration. Furthermore, CCL3 expression was elevated in the plasma of patients with MCL as compared with normal control participants consistent with our earlier finding that serum CCL3 levels are elevated in MCL tumors.[33] In fact, high plasma levels of CCL3 were associated with poor survival rates in CLL and diffuse large B-cell lymphoma, suggesting the important role of CCL3 in other B-cell malignancies.[38] Chemokines, including CCL3, are promiscuous in their use of chemokine receptors CCR1 and CCR5, allowing for a complex interactome. We identified that CCR1 is highly expressed on monocytes and BMDM but to a lesser degree on MCL cell lines or MCL tumors. These results suggest that the CCL3-CCR1 axis exerts its effects on monocytes/macrophages in a paracrine manner. Again, these observations cannot rule out the possibility of an autocrine CCL3-CCR1 axis playing some role.

We took advantage of the CCR1 antagonist, CCR1 siRNA, and *CCR1 KO* mice to explore this axis. *CCR1-/-* immunocompetent mice showed a reduced migration of thioglycolate-stimulated PEM and BMDM stimulated with MCL-CM or with rCCL3. Furthermore, the CCR1 inhibitor BX-471 or CCR1 siRNA, but not the CCR5 inhibitor maraviroc, significantly reduced THP1 or $CD14^+$ Mo migration induced by MCL-CM. This study is in contrast to a study on Hodgkin lymphoma (HL) in which CCR5 antagonists inhibit the HL and TME interactions,[39] which may not be surprising given the pleomorphic TME in HL. This study is consistent with a study that has shown that CSF1R inhibition disrupts the dialogue between MCL and macrophages.[40]

In conclusion, our studies revealed a novel mechanism of TAMs programming using in vitro and in vivo MCL models including samples of patients with MCL. Our findings propose that autocrine secretion of CCL3 from MCL tumor promotes monocyte/macrophage recruitment and macrophage polarization to M2-phenotype by increasing IL-10 expression/secretion. In turn, M2-TAM–produced IL-10 increased the CCL3 secretion for continuous migration of macrophages to MCL-TME; these 2 important events were connected via CCR1, which is highly expressed on the TAMs (visual abstract). These novel mechanistic findings raise the possibility of clinically targeting this CCL3-CCR1 axis with CCR1 antagonists by reshaping the lymphoma-TME. Such insights could be critical for designing more effective targeted combination therapies such as BTK or BCL2 inhibitors or immune therapies to improve clinical responses in MCL and perhaps other B-cell lymphoma subtypes.

Acknowledgment

This work was supported by start-up funding from George Washington University, GW Cancer Center (M.G.).

Authorship

Contribution: K.L. and J.S. conducted the experiments, acquired data, analyzed the data, and made the figures; J.G. performed bioinformatics analysis; M.S. provided the murine MCL cell line and edited the manuscript; W.K.E. provided BM and BMDM from *IL-10* KO and WT mice; T.P. provided MCL clinical samples and MCL plasma; M.G. conceived and designed the study, interpreted the data, wrote the manuscript, and finalized the figures; and all authors reviewed and approved the manuscript.

Conflict-of-interest disclosure: The authors declare no competing financial interests.

ORCID profiles: T.P., 0000-0003-2143-9672; M.G., 0000-0003-2081-3941.

Correspondence: Mamta Gupta, Department of Biochemistry and Molecular Medicine, School of Medicine and Health Sciences, George Washington University, GW Cancer Center, Washington DC, 20052; email: magupta@gwu.edu.

Figure 7 (continued) (green) antibodies. Nuclei were stained with DAPI (blue). (F) Immunofluorescent staining was performed on the syngeneic mouse tumor using a CD8 antibody (red). (G-H) Bar diagram of the relative percentage of $CD206^+$ to $F4/80^+$ cells in control and CCR1 inhibitor–treated groups (G); Bar diagram representing the percentage of $CD8^+$ T cell infiltration (H). Data represent the mean of the 5 to 10 microscopic fields. All staining was performed on at least 3 mouse tumors and a representative image is shown.

References

1. Dreyling M, Campo E, Hermine O, et al. Newly diagnosed and relapsed mantle cell lymphoma: ESMO Clinical Practice Guidelines for diagnosis, treatment and follow-up. *Ann Oncol*. 2017;28(suppl_4):iv62-iv71.
2. Dreyling M, Aurer I, Cortelazzo S, et al. Treatment for patients with relapsed/refractory mantle cell lymphoma: European-based recommendations. *Leuk Lymphoma*. 2018;59(8):1814-1828.
3. Vose JM. Mantle cell lymphoma: 2017 update on diagnosis, risk-stratification, and clinical management. *Am J Hematol*. 2017;92(8):806-813.
4. Romaguera JE, Fayad L, Rodriguez MA, et al. High rate of durable remissions after treatment of newly diagnosed aggressive mantle-cell lymphoma with rituximab plus hyper-CVAD alternating with rituximab plus high-dose methotrexate and cytarabine. *J Clin Oncol*. 2005;23(28):7013-7023.
5. Delarue R, Haioun C, Ribrag V, et al. CHOP and DHAP plus rituximab followed by autologous stem cell transplantation in mantle cell lymphoma: a phase 2 study from the Groupe d'Etude des Lymphomes de l'Adulte. *Blood*. 2013;121(1):48-53.
6. Le Gouill S, Thieblemont C, Oberic L, et al. Rituximab after Autologous Stem-Cell Transplantation in Mantle-Cell Lymphoma. *N Engl J Med*. 2017; 377(13):1250-1260.
7. Goy A, Bernstein SH, Kahl BS, et al. Bortezomib in patients with relapsed or refractory mantle cell lymphoma: updated time-to-event analyses of the multicenter phase 2 PINNACLE study. *Ann Oncol*. 2009;20(3):520-525.
8. Rule S, Dreyling M, Goy A, et al. Ibrutinib for the treatment of relapsed/refractory mantle cell lymphoma: extended 3.5-year follow up from a pooled analysis. *Haematologica*. 2019;104(5):e211-e214.
9. Zhao S, Kanagal-Shamanna R, Navsaria L, et al. Efficacy of venetoclax in high risk relapsed mantle cell lymphoma (MCL) - outcomes and mutation profile from venetoclax resistant MCL patients. *Am J Hematol*. 2020;95(6):623-629.
10. Zhao X, Wang MY, Jiang H, et al. Transcriptional programming drives Ibrutinib-resistance evolution in mantle cell lymphoma. *Cell Rep*. 2021;34(11): 108870.
11. Chiron D, Bellanger C, Papin A, et al. Rational targeted therapies to overcome microenvironment-dependent expansion of mantle cell lymphoma. *Blood*. 2016;128(24):2808-2818.
12. Chen Z, Teo AE, McCarty N. ROS-Induced CXCR4 signaling regulates mantle cell lymphoma (MCL) cell survival and drug resistance in the bone marrow microenvironment via autophagy. *Clin Cancer Res*. 2016;22(1):187-199.
13. Noy R, Pollard JW. Tumor-associated macrophages: from mechanisms to therapy. *Immunity*. 2014;41(1):49-61.
14. Qian BZ, Pollard JW. Macrophage diversity enhances tumor progression and metastasis. *Cell*. 2010;141(1):39-51.
15. Gonzalez H, Hagerling C, Werb Z. Roles of the immune system in cancer: from tumor initiation to metastatic progression. *Genes Dev*. 2018;32(19-20): 1267-1284.
16. Chen Y, Song Y, Du W, Gong L, Chang H, Zou Z. Tumor-associated macrophages: an accomplice in solid tumor progression. *J Biomed Sci*. 2019; 26(1):78.
17. Song K, Herzog BH, Sheng M, et al. Lenalidomide inhibits lymphangiogenesis in preclinical models of mantle cell lymphoma. *Cancer Res*. 2013;73(24): 7254-7264.
18. Pham LV, Vang MT, Tamayo AT, et al. Involvement of tumor-associated macrophage activation in vitro during development of a novel mantle cell lymphoma cell line, PF-1, derived from a typical patient with relapsed disease. *Leuk Lymphoma*. 2015;56(1):186-193.
19. Le K, Sun J, Khawaja H, et al. Mantle cell lymphoma polarizes tumor-associated macrophages into M2-like macrophages, which in turn promote tumorigenesis. *Blood Adv*. 2021;5(14):2863-2878.
20. Schall TJ, Proudfoot AE. Overcoming hurdles in developing successful drugs targeting chemokine receptors. *Nat Rev Immunol*. 2011;11(5):355-363.
21. Griffith JW, Sokol CL, Luster AD. Chemokines and chemokine receptors: positioning cells for host defense and immunity. *Annu Rev Immunol*. 2014;32: 659-702.
22. Charo IF, Ransohoff RM. The many roles of chemokines and chemokine receptors in inflammation. *N Engl J Med*. 2006;354(6):610-621.
23. Godessart N. Chemokine receptors: attractive targets for drug discovery. *Ann N Y Acad Sci*. 2005;1051:647-657.
24. Lentzsch S, Gries M, Janz M, Bargou R, Dorken B, Mapara MY. Macrophage inflammatory protein 1-alpha (MIP-1 alpha) triggers migration and signaling cascades mediating survival and proliferation in multiple myeloma (MM) cells. *Blood*. 2003;101(9):3568-3573.
25. Li YL, Shi ZH, Wang X, Gu KS, Zhai ZM. Prognostic significance of monocyte chemoattractant protein-1 and CC chemokine receptor 2 in diffuse large B cell lymphoma. *Ann Hematol*. 2019;98(2):413-422.
26. Yu X, Huang Y, Collin-Osdoby P, Osdoby P. CCR1 chemokines promote the chemotactic recruitment, RANKL development, and motility of osteoclasts and are induced by inflammatory cytokines in osteoblasts. *J Bone Miner Res*. 2004;19(12):2065-2077.
27. Ishida N, Hayashi K, Hattori A, Yogo K, Kimura T, Takeya T. CCR1 acts downstream of NFAT2 in osteoclastogenesis and enhances cell migration. *J Bone Miner Res*. 2006;21(1):48-57.
28. Smith MR, Joshi I, Pei J, et al. Murine mantle cell lymphoma model cell line. *Leukemia*. 2013;27(7):1592-1594.
29. Wilcox RA, Wada DA, Ziesmer SC, et al. Monocytes promote tumor cell survival in T-cell lymphoproliferative disorders and are impaired in their ability to differentiate into mature dendritic cells. *Blood*. 2009;114(14):2936-2944.

30. Le K, Wellik LE, Maurer MJ, McPhail ED, Witzig TE, Gupta M. JAK2 activation promotes tumorigenesis in ALK-negative anaplastic large cell lymphoma via regulating oncogenic STAT1-PVT1 lncRNA axis. *Blood Cancer J*. 2021;11(3):56.

31. Demosthenous C, Gupta SK, Sun J, Wang Y, Troska TP, Gupta M. Deregulation of polycomb repressive complex-2 in mantle cell lymphoma confers growth advantage by epigenetic suppression of cdkn2b. *Front Oncol*. 2020;10:1226.

32. Basso K, Margolin AA, Stolovitzky G, Klein U, Dalla-Favera R, Califano A. Reverse engineering of regulatory networks in human B cells. *Nat Genet*. 2005;37(4):382-390.

33. Sonbol MB, Maurer MJ, Stenson MJ, et al. Elevated soluble IL-2Ralpha, IL-8, and MIP-1beta levels are associated with inferior outcome and are independent of MIPI score in patients with mantle cell lymphoma. *Am J Hematol*. 2014;89(12):E223-E227.

34. Ouyang W, Rutz S, Crellin NK, Valdez PA, Hymowitz SG. Regulation and functions of the IL-10 family of cytokines in inflammation and disease. *Annu Rev Immunol*. 2011;29:71-109.

35. von Haehling S, Wolk K, Hoflich C, et al. Interleukin-10 receptor-1 expression in monocyte-derived antigen-presenting cell populations: dendritic cells partially escape from IL-10's inhibitory mechanisms. *Genes Immun*. 2015;16(5):366.

36. Boissard F, Fournie JJ, Laurent C, Poupot M, Ysebaert L. Nurse like cells: chronic lymphocytic leukemia associated macrophages. *Leuk Lymphoma*. 2015;56(5):1570-1572.

37. Serbina NV, Jia T, Hohl TM, Pamer EG. Monocyte-mediated defense against microbial pathogens. *Annu Rev Immunol*. 2008;26:421-452.

38. Takahashi K, Sivina M, Hoellenriegel J, et al. CCL3 and CCL4 are biomarkers for B cell receptor pathway activation and prognostic serum markers in diffuse large B cell lymphoma. *Br J Haematol*. 2015;171(5):726-735.

39. Casagrande N, Borghese C, Visser L, Mongiat M, Colombatti A, Aldinucci D. CCR5 antagonism by maraviroc inhibits Hodgkin lymphoma microenvironment interactions and xenograft growth. *Haematologica*. 2019;104(3):564-575.

40. Papin A, Tessoulin B, Bellanger C, et al. CSF1R and BTK inhibitions as novel strategies to disrupt the dialog between mantle cell lymphoma and macrophages. *Leukemia*. 2019;33(10):2442-2453.